Representation of Forest Cover in a Physically Based Snowmelt Model, Phase I

R.Å. HELLSTRÖM[1]

ABSTRACT

This project develops a pragmatic procedure for measuring and modeling the effects of forest cover on snowdepth, thus facilitating improvement of an existing state-of-the-art snowmelt model. The first of two Phases develops sub-models and provides empirical results of their independent evaluation. Four numerical schemes modify the magnitude of longwave and shortwave radiation, precipitation and wind speed beneath different types of forest cover. The University of Michigan Biological Station, provided a pine and deciduous site and some resources for meteorological observations from the AmeriFlux and PROPHET towers. Two unique automatic weather stations provided most of the data to necessary for verification of the models. Results indicate good agreement between the solar radiation and wind sub-models compared to measurements, although insufficient field resources precluded validation of the longwave radiation and precipitation schemes. Nevertheless, comparison with above canopy observations of snowfall and modeled longwave radiation suggest realistic trends in the latter two sub-models.

KEY WORDS snowdepth; northern hardwood forest; physically-based models; leaf area index

INTRODUCTION

Estimating the temporal and spatial variations of seasonal snow cover beneath a region with heterogeneous forest is advancing through application of forest cover parameterizations that estimate the radiation budget at the snow surface. Modeling and field studies suggest the following energy and mass balance trends at the ground beneath the forest cover, all relative to above-canopy values or a near-by, open location (Berry and Rothwell, 1992; Yamazaki and Kondo, 1992; Ni et al., 1997):

1. decrease in incoming shortwave radiation $K\downarrow$ at the forest floor,
2. increase in incoming longwave radiation $L\downarrow$,
3. decrease in wind speed leading to reduced turbulent sensible Q_h and latent Q_e heat exchange between the atmosphere and ground, and
4. decrease in precipitation P accumulated at the forest floor.

Of these four effects, it is apparent that current advances in physically based models seem to focus on factors 1 and 2, which are required for determining the net radiation Q^*, and are commonly regarded as the primary source of energy for snowmelt. However, observational and modeling studies suggest significant turbulent sensible Q_h and latent Q_e heat exchange at the snow surface for regions lying in the path of wintertime storm tracks, or locations otherwise experiencing episodes of warm and cold air advection (horizontal wind flow) (Male and Granger, 1981). Since Q_h can be up to twice the magnitude of Q^* and Q_e can equal Q^*, Morris (1989)

[1] Department of Geography, The Ohio State University, 1036 Derby Hall, Columbus, Ohio 43210-1361, U.S.A

suggested that it is critical for snowmelt modelers to measure or calculate the sensible heat flux and evaporation with at least the same level of precision as is possible for net radiation. Thus, since the amount of turbulent heat flux is proportional to the wind speed, it is important to accurately simulate factor 3, particularly for applications in the mid-latitudes, where the passage of storms frequently causes shifts in wind direction and speed. The bluff-body effect of the forest canopy architecture substantially reduces wind speed below that above the canopy or at an open site. Hence, it would be important to estimate factor 3, particularly for applications in distributed modeling of regions with heterogeneous land cover. In addition, the stability of the air within the canopy must be properly estimated to determine turbulent heat exchange. Furthermore, physically based snowmelt models often consider the processes of snow accumulation and drifting (Tarboton and Luce, 1997). Variability in canopy architecture or gaps between clumps of vegetation may substantially affect snow depth through factor 4. This project builds upon the success of earlier parameterizations to produce practical, physically based parameterizations (henceforth referred to as sub-models) of sub-canopy radiation (factors 1 and 2), wind speed (factor 3) and precipitation interception (factor 4). Each sub-model is designed so that it may be coupled into physically based snowmelt models such as the Utah Energy Balance snow accumulation and melt (UEB) model (Tarboton and Luce, 1997) or SNTHERM (Jordan, 1991).

This paper reports on the initial results of a two-phase empirical and modeling study. Phase I, presented herein, estimates the sub-canopy energy and water budgets from standard (hourly) meteorological observations and widely used parameters that distinguish different types of forest canopy architecture. Models were compared against measurements from unique micrometeorological measurement systems established at the University of Michigan Biological Station (UMBS), 45°35'N, 84°42'W, 324 m above sea level. UMBS is located near Pellston, MI, which is appropriately labeled as the "Icebox of the Nation". UMBS maintains extensive plots of mature northern hardwood forest and a recently installed AmeriFlux tower, thus providing the data necessary for completion of all phases of this project. A red pine and mixed deciduous site provided striking evidence of the effects of different types of forest cover on factors 1 through 4. Phase II, with an expected completion date in August, 1999, will integrate the four sub-models, independently and in various combinations, into a state-of-the-art snowmelt model.

THE SUB-MODELS

Each new version of the UEB model will incorporate individual modifications to the radiation balance, wind speed and precipitation schemes. The leaf area index (LAI) and sky view factor (SVF) are standard parameters that represent the amount of vegetation and provide good estimates of the fractional penetration of solar and emission of terrestrial radiation. The term SVF represents the weighted canopy openness, which is based on the fraction of the total number of open pixels on a sky hemisphere divided by the total number possible for the unobstructed sky (Chazdon and Field, 1987). Nel and Wessman (1993) and Fassnacht et al. (1994) suggested simplistic geometrical-optical methods, while Li et al. (1995) developed a new, more elaborate, technique that combines geometrical-optical and radiation transfer methods. Both methods incorporate the LAI or SVF. In addition to altering the radiation balance, field observations suggest that forest architecture changes the precipitation (McKay and Gray, 1981) and the wind speed (Szeicz et al., 1979; Ni, 1997) relative to an open location. The advantage of the LAI and SVF parameters is that they are relatively easy to measure for any type of vegetation including crops and forest cover. All sub-models were developed from proven schemes available in the literature. Figs. 1 and 2 indicate the effects of forest cover on the mass and energy balance at the forest floor.

The mass balance of the snowpack is given by

$$S = P - I - E - M - F. \quad (1)$$

where S is the rate of change in snow depth (SWE m hr^{-1}), P is the precipitation (SWE m hr^{-1}), I is precipitation intercepted by the forest canopy (SWE m hr^{-1}), E is the evaporation-sublimation rate (m hr^{-1}), M is the melt rate (m hr^{-1}) and F is the infiltration rate (m hr^{-1}). The UEB model combines the values of M and F into a single meltwater term.

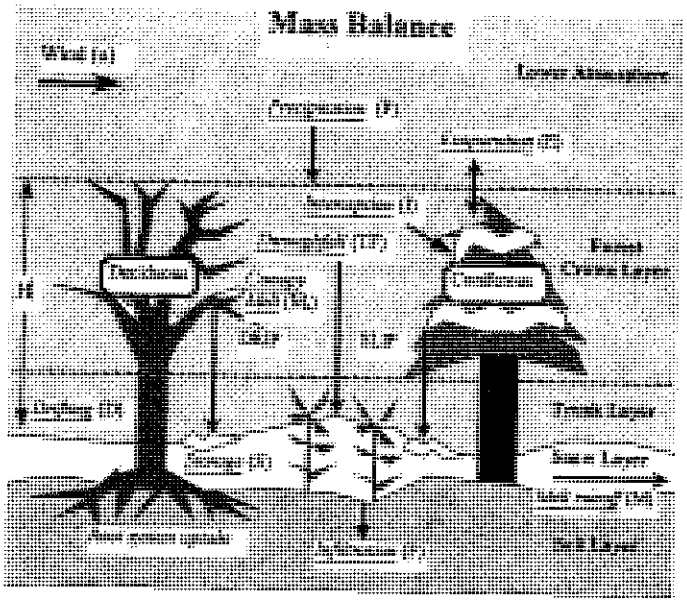

Figure 1. Processes affecting the mass balance beneath the forest.

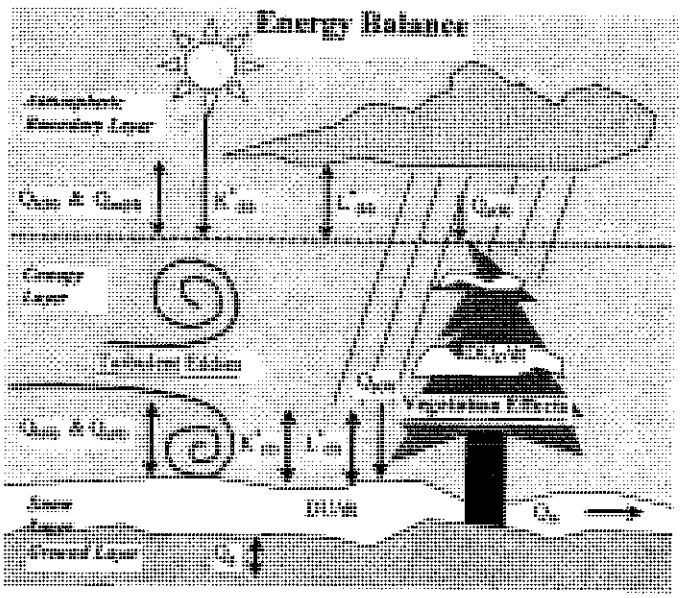

Figure 2. Processes affecting the energy balance beneath the forest canopy.

The energy balance of the snowpack is given by

$$DU/dt = K^*_{(0)} + L^*_{(0)} + Q_{e(0)} + Q_{h(0)} + Q_g + Q_{p(0)} - Q_m \qquad (2)$$

where the last three variables represent the substrate heat flux Q_g, heat advected by precipitation $Q_{p(0)}$ and heat lost through melt water output from the snowpack Q_m. All terms share flux density units (kJ m^{-2} hr^{-1}).

Shortwave radiation at the forest floor

Sub-models estimating incoming shortwave and longwave radiation incorporate measured values of vegetation area index (VAI) at the two forest sites. The VAI represents the vegetation

area per unit forest floor area, where the vegetation area is accumulated from the top of the canopy at level z = H to the level of the snow surface z = 0. During daylight hours (ranging between 8 and 9 hours during the snow season in northern Michigan) with clear skies, the attenuation by forest structure decreases the amount of solar irradiance when compared to an open site. Thus, an increase in VAI is expected to decrease the solar radiation input to snow cover by day. Under clear sky conditions by night and daylight, the forest canopy effectively combines the sky and forest canopy emissivity, thereby increasing the downward-directed terrestrial radiative transfer to the snow. The effects of forest cover on radiation will be modeled from a variation on Beer's law for solar and application of the SVF for longwave radiation.

The Beer-Lambert Law (Monsi and Saeki, 1953), which assumes random distribution of leaves and branches in space, expresses the incoming solar radiation penetrating the canopy to the forest floor with the formulation

$$K\downarrow_{(0)} = K\downarrow_{(H)}\exp(-a_v VAI). \quad (3)$$

where a_v is the light extinction coefficient of a particular type of vegetation and $K\downarrow_{(H)}$ is the above canopy irradiance, which was continuously measured by a Li-COR pyranometer fixed at the 46 m level of the AmeriFlux tower. Nel and Wessman (1993) discussed the relationships between VAI and solar radiation. According to Norman (1979), the extinction coefficient represents the fraction of leaf area projected onto a horizontal surface and its magnitude is sun angle dependent (Pierce and Running, 1988). The simplest expression for a_v assumes an average value for a certain species of vegetation. For example, Jarvis and Leverenz (1983) found an average value of $a_v = 0.5$ for coniferous forest cover. Monteith (1976) provides a_v values for coniferous and deciduous forest species with a theoretical range between 0 and 1.

An alternative equation for $K\downarrow_{(0)}$ permits a_v to change with solar zenith angle Z. Micrometeorological measurements indicate a significant dependence between a_v and Z, with maximum values of a_v occurring at low solar elevations between 15° and 20° (Monteith, 1976). Nel and Wessman (1993) compared different methods of estimating VAI and found that including solar zenith angle dependence did not significantly improve the results. For example, Campbell and Norman (1989) evaluated a theoretical value of a_v based on a spherical leaf angle distribution:

$$a_v = 1/(2\cos Z). \quad (4)$$

This formula gives a minimum value of $a_v = 0.5$ when the Sun is directly overhead, which is within the measured range of maximum coniferous a_v values reported by Jarvis and Leverenz (1983), 0.40 to 0.65. From Eq. 4, the maximum theoretical range of a_v for the snow season at UMBS would be from 0.67 on 31 March to ∞ at sunrise and sunset. Fassnacht et al. (1994) suggest obtaining a_v values from the literature. Monteith (1976) provides some measured values of a_v, although a more extensive list is expected. Nevertheless, it appears that some physics-based modeling studies apply equations similar to Eq. 4 with reasonable results (Pomeroy et al., 1998); hence, it will be incorporated into the solar radiation scheme. Note: the factor 2 in the denominator of Eq. 4 was adjusted to 2.5 for the VAI>1. for subsequent analysis. This improved results.

Longwave radiation at the forest floor

For longwave irradiance at the snow surface, both sky $L\downarrow_{(H)}$ and vegetation canopy $L\downarrow_C$ contribute, so that

$$L\downarrow_{(0)} = L\downarrow_C(1\text{-SVF}) + L\downarrow_{(H)}\text{SVF}. \quad (5)$$

where the value of $L\downarrow_C$ would be estimated from temperature T_C measured, ideally, at the level of maximum crown density, but, in this project, estimated by the above-canopy air temperature, represented by

$$L\downarrow_C = \sigma\varepsilon_C T_C^4. \quad (6)$$

where emissivity $\varepsilon_C = 1$ is assumed for trees, thus the longwave irradiance is

$$L\downarrow_{(0)} = \sigma T_C^4(1\text{-SVF}) + L\downarrow_{(H)}\text{SVF}. \quad (7)$$

The value of $L\downarrow_{(H)}$ is that available within the UEB model, measured or estimated, based on the transmissivity of the atmosphere (Tarboton and Luce, 1997).

Sub-canopy wind speed

The mean wind speed within the canopy and at the forest floor is reduced (Lee, 1978). Measurements indicate that wind speed within forest canopies increases only slightly from the 1.5-m level up to the level of maximum crown density, above which wind speed increases at a much greater rate (Monteith, 1976; Ni, 1997).

This project incorporates the work of Meyers et al. (1998), who successfully applied a sub-canopy wind formulation developed by Cionco (1972). Cionco utilizes values of VAI and its vertical distribution to define sub-canopy wind speed as

$$u(z) = u(H)\exp(-\text{VAI}(1 - z/H)^{\beta}). \quad (8)$$

β is a wind profile fitting coefficient:

$$\beta = 1 - (F - 1)/4. \quad (9)$$

where F is an integer indicating one of three basic VAI profiles; F = 1 for young pine, F = 2 for leafed deciduous, and F = 3 for old pine with long stems and clumping at the top. Note: the exponential term was multiplied by a factor of 2 for VAI<1.0 and a factor of 0.75 for VAI>2.0. This improved estimations of wind speed (see next section). The term u(H) is estimated from the log-linear relationship (Meyers et al., 1998),

$$u(H) = (u^*/k)\ln[(H-d+z_0)/z_0] \quad (10)$$

where u^* is the friction velocity (calculated from Nickerson and Smiley, 1975; Benoit, 1977) and d and z_0 are defined by Meyers et al. (1998) as,

$$d = H[0.05 + \text{VAI}^{0.2}/2 + (F - 1)/20] \quad (11)$$

$$z_0 = H[0.23 + \text{VAI}^{0.25}/10 - (F - 1)/67] \quad (12)$$

If z_0 is less than 1, z_0 is set equal to 0.1H. Two advantages of this formulation are that it satisfies the goal of utilizing VAI in the wind sub-model and it accounts, to some extent, for vertical differences in canopy structure that will likely influence wind distribution. The wind sub-model requires three input parameters for each forest type, including VAI, H and F.

Precipitation at the forest floor

The mass balance scheme of many snowmelt models, including the UEB model (Tarboton and Luce, 1997) and SNTHERM (Jordan, 1991), do not include forest interception, so that their distribution over basins with heterogeneous forest cover is not advisable, particularly for simulation of abrupt accumulation and melt events. The original UEB model version, separates precipitation P into snow P_S or rain P_R depending on the air temperature and alters its distribution with the drift factor DF. Because of this and the fact that a few periods of rainfall are possible during the winter season at UMBS, this project will consider the effects of forest cover on rainfall and snowfall. Furthermore, interception is likely dependent upon wind speed, which enhances rainfall drip and snow slip, thus depleting the canopy storage and adding to the accumulation at the forest floor. Hörmann et al. (1996) found that a considerable amount of precipitation (rainfall in this case) is shaken out of the crown by the wind. Consequently, they developed a statistical relationship between canopy storage capacity and wind speed, although the correlation coefficient

between the two was rather low at $r^2 = 0.4$. Nevertheless, their results show that wind speeds in excess of 3 m s^{-1} reduced canopy storage by a factor of two or greater. This suggests that wind significantly effects the amount of precipitation reaching the forest floor and therefore its effects will be introduced into the precipitation sub-model. Preliminary observations at UMBS indicate substantial snow and rain interception, especially in the pine forest, and wind speeds greater than 3 m s^{-1} substantially increase drip and slip to the snow surface. This section formulates a sub-model that explicitly incorporates VAI, SVF and wind speed.

The classic mass balance represents throughfall TF as

$$TF = P - I - SF. \tag{13}$$

where SF is the stem flow of rain or melt water. The term SF is relatively small and is commonly omitted to simplify the mass balance estimations. Eq. 13 does not explicitly consider processes that reduce the storage of intercepted precipitation, specifically evaporation, sublimation, rain drip and snow slip. Each leaf, needle or branch on a tree has a surface area, which may be exposed to falling precipitation. Initially, the throughfall would be low, as the canopy biomass effectively intercepts precipitation, and with time, evaporation, and forces of gravity and wind will deplete the canopy storage. The challenge is to derive a formulation for I in terms of VAI and/or SVF. Most studies suggest using empirical expressions, but this work will rely on physically based formulations.

Compared to an open control site, forest structure, including stems and leaves (or needles), intercepts a percentage of snowfall reaching the forest floor. Since the VAI estimates the area of the branches and leaves in the canopy per unit area of forest floor, it provides an index of the area of potential interception. A box model illustrates the storage and flow of liquid and solid precipitation between a reservoir source in the atmosphere and sink at the canopy floor. The objective is to estimate the amount of accumulated precipitation at the canopy floor. Fig. 3 illustrates how above-canopy precipitation flows through the forest canopy and the processes affecting the amount that eventually reaches the ground.

This conceptual model accounts for the effects of forest cover on the water budget at the forest floor. All fluxes have units of depth per unit time (per unit surface area). The primary objective is to determine the amount of precipitation that penetrates or leaves the canopy layer to reach the ground, designated P_G. The input variables for the interception sub-model include, forest canopy architecture (VAI and Sky View Factor, SVF), and above canopy (or open site) measurements of precipitation as rain P_R or snow P_S, air temperature, relative humidity and wind speed. The output variables include hourly estimates of the portion of liquid and solid precipitation that is intercepted by the canopy, lost to the atmosphere and ultimately accumulated at the ground.

The vast majority of precipitation-and-vegetation modeling research considers only processes controlling the flows of liquid precipitation through the canopy. The prominent interception models include those of Rutter et al. (1971), Gash (1979), Massman (1983) and Calder (1986). In addition, purely empirical models, such as that of Helvey and Patrick (1965), have applications to specific types of forest cover. The model developed herein will incorporate the processes developed in the physics-based rainfall models with modifications for snowfall. Many recent studies are based on the predictive rainfall model developed by Rutter et al. (1971). This model does not consider solid precipitation, specifically snow, although it provides a sound physical basis for designing such a model. Some examples of successful integration of the Rutter model include those of Domingo et al. (1998), Lundberg et al. (1998), and Hörmann et al. (1996).

The interception sub-model is formulated according to Fig. 3. The sub-model estimates the precipitation reaching the ground, $P_{G(S)}$ for snow and $P_{G(R)}$ for rain as

$$P_{G(R)} = TF_R + DRIP \text{ and} \tag{14}$$

$$P_{G(S)} = TF_S + SLIP. \tag{15}$$

where the snow or rain throughfall TF_S and TF_R are calculated from the SVF parameter and snow or rain inputs P_S and P_R,

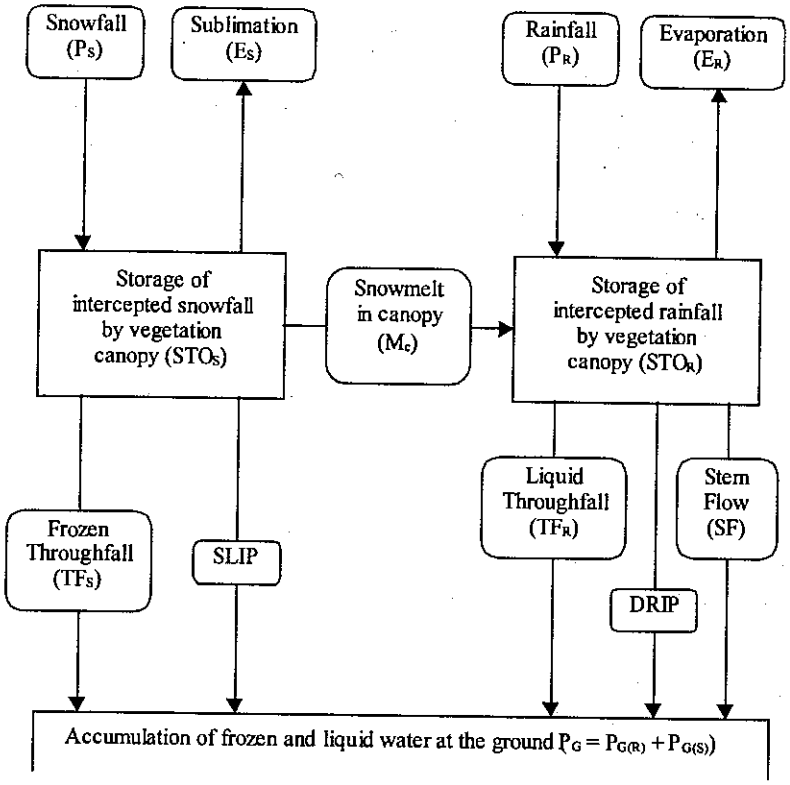

Figure 3. Conceptual interception sub-model indicating storage, sources, sinks and flow of water in a forest canopy system.

$$TF_R = P_R SVF \text{ and} \tag{16}$$
$$TF_S = P_S SVF, \tag{17}$$

which falls directly to the ground, so that the intercepted rain I_R and snow I_S are the remaining portion of P_R and P_S,

$$I_R = P_R(1 - SVF) \text{ and} \tag{18}$$

$$I_S = P_S(1 - SVF). \tag{19}$$

Next, the dynamic components of storage, DRIP and SLIP are determined based on melt criteria, storage capacity estimations and critical wind speed. Tarboton and Luce (1997) derived a formula for latent heat flux toward the snow surface:

$$Q_e = \rho_a L_s (q_a - q_s)/r_a. \tag{20}$$

where r_a (hr m^{-1}) is the aerodynamic resistance to vapor transport, which depends on boundary layer stability. Lowe (1977) defines the saturation vapor pressure e_s at the snow surface by assuming it is saturated at T_s; hence the Clausius-Clapeyron equation holds for specific humidity:

$$dq/dT_a = 0.622\, L_v \bar{q}_s /(R_d \bar{T}_a^2). \tag{21}$$

where 0.622 is the ratio of the gas constants for water vapor to dry air (often represented by ϵ), and the overbar denotes the temporal mean value. The term $R_d = 287$ J kg^{-1} K^{-1} is the gas constant for dry air. The saturation specific humidity q_s relates to the saturation vapor pressure and atmospheric pressure P_a:

$$q_s = 0.622\ (e_s/p_a). \tag{22}$$

Lowe (1977) provides polynomial approximations for the saturation vapor pressure over water and ice. Applying the ideal gas law, $p_a = \rho_a R_d T_a$, and replacing the specific humidity difference by vapor pressure, Eq. 20 takes the form:

$$Q_e = 0.622 L_s(e_a - e_s(T_s))/(r_a R_d T_a). \tag{23}$$

The rate of evaporation is,

$$E = (0.622(e_a - e_s(T_s))/(r_a R_d T_a) \qquad (kg\ m^{-2}\ hr^{-1}) \tag{24}$$

To get the depth rate of evaporation, E is divided by the density of water, so that,

$$E = (0.622(e_a - e_s(T_s))/(r_a \rho_w R_d T_a) \quad (m\ hr^{-1}) \tag{25}$$

The sources, flows and sinks of precipitation are estimated from the following formulation. First, if snow is stored in the canopy, it may melt and the criteria for snowmelt will depend on the same critical air temperatures that Tarboton and Luce (1997) devised to delineate between snowfall T_{sn} and rainfall T_m:

If $T_a \le T_{sn}$ (All Snow)

$$STO_S(t) = STO_S(t\text{-}dt) + P_S(1 - SVF) - M_C(t\text{-}dt) - SLIP - E_S \tag{26}$$

$$E_S = -VAI[0.622(e_a - e_{si})/(r_{aS}\rho_w R_d T_a(K))] \tag{27}$$

$$SLIP = STO_S \exp(-u_{crit} VAI/u_0) \tag{28}$$

If $T_a \ge T_m$ (All Rain or Melt)

$$STO_R(t) = STO_R(t\text{-}dt) + P_R(1 - SVF) + M_C(t) - DRIP - E_R \tag{29}$$

$$E_R = -VAI[0.622(e_a - e_s)/(r_{aR}\rho_w R_d T_a(K))] \tag{30}$$

$$DRIP = STO_R \exp(-u_{crit} VAI/u_0) \tag{31}$$

If $STO_S > 0$ $\quad M_c = (Q^*_{(H)} + Q_P - Q_{h(H)} - Q_{e(H)})/(\rho_w L_f)$ (32)

If $T_{sn} < T_a < T_m$ Both SLIP and DRIP components of storage are estimated

The internal energy of the snow stored within the canopy Q_{Mc} is included in the M_c term, since it is assumed that all intercepted snow eventually leaves the canopy. The first term on the right hand side of Eq. 32 is the net radiation, which is the sum of the net solar $K^*_{(H)}$ and longwave $L^*_{(H)}$ radiation at the canopy-atmosphere interface, and

$$K^*_c = K{\downarrow}_0(1 - \alpha_c), \tag{33}$$

where the canopy albedo α_c depends on solar elevation and proportion of canopy covered with snow. For defoliated birch-aspen forest, the albedo ranges from 0.26 with a solar elevation of 40° to 0.31 with a solar elevation of 10° (Monteith, 1976). For pine forest, the albedo ranges from 0.1 with a solar elevation of 40° to 0.15 for a solar elevation of 10° (Monteith, 1976), but may be greater with snow stored in the canopy. Pomeroy and Dion (1996) described pine canopies as 'light-traps' that effectively eliminate albedo enhancement due to intercepted snow. Observations at UMBS indicate that wind substantially reduces the amount of snow storage, particularly in the upper third of the canopy, so the elevated albedo due to snow interception is likely short-lived (at most a day or two). Furthermore, the forest elements encourage multiple reflections, thus keeping the effective albedo lower than would be expected for a flat surface with snow cover.

The magnitudes of $L^*_{(H)}$, $Q_{e(H)}$, and $Q_{h(H)}$ are given by

$$L^*_{(H)} = L{\downarrow}_0 - \sigma\varepsilon_c T_c^4 \tag{34}$$

$$Q_{e(H)} = E_R L_v \tag{35}$$

$$Q_{h(H)} = (\rho_a c_p / r_{aRc})(T_a - T_c) = 0 \qquad (36)$$

It is often assumed that $T_a = T_c$, since the difference between the canopy and air temperature for deciduous and coniferous trees is likely less than 0.5 degrees, particularly for wind speeds greater than 1 m s^{-1} (Monteith, 1976; Yomaoka, 1958). Therefore, $Q_{h(H)} = 0$ for this interception sub-model. The same formulation applied to the snowpack in the original UEB model (Tarboton and Luce, 1997), provides the heat advected from precipitation, so that the canopy storage of snow receives

$$Q_{p(H)} = P_{s(H)} c_s \rho_w [\min(T_a, 0°C)] + P_{r(H)}(L_f \rho_w + c_w \rho_w [\max(T_a, 0°C)]) \qquad (37)$$

where min and max are operators on the variables in parentheses.

The aerodynamic resistance for evaporation r_{aR} assumes a neutral profile, so that,

$$r_{aRn} = (1/k^2 u)[\ln(z - d)/(z_0)]^2 \qquad (38)$$

where d and z_0 were defined by Eqs. 11 and 12. Knowing the value of r_{aRn}, many studies consider the work of Calder (1990) to estimate the aerodynamic resistance for snow as

$$r_{aSn} = 10 r_{aRn} \qquad (39)$$

which results largely because of the smoothness of snow in the canopy and less surface area (per unit volume) exposed to airflow.

Precipitation interception changes the storage of rain and snow within the canopy. This sub-model assumes that the maximum possible storage is equal to the storage capacity CAP of the particular type of vegetation. The limits on storage capacities are, $0 < STO_R < CAP_R$ for rainfall and $0 < STO_S < CAP_S$ for snowfall. Lee (1980) and Monteith (1975) provide a review of the mechanisms governing canopy interception, and both indicate a wide range for CAP_R and CAP_S depending on storm frequency (related to the density of snow and degree of saturation by rainfall) and vegetation type. A formulation to estimate storage capacity should consider the quality of snow (often represented by its density) and the canopy architecture (represented by VAI). Hedström and Pomeroy (1998) applied the formulation of Schmidt and Gluns (1991) to estimate the canopy snow load SNLOAD for a particular type of vegetation

$$SNLOAD = VAI[SNLOAD_{branch}(0.27 + 46/\rho_{snow})] \qquad (kg\ m^{-2}) \qquad (40)$$

where the fresh snow density is estimated by the US Army Corps of Engineers (1956) as

$$\rho_{snow} = 67.92 + 51.25\exp(T_a/2.59) \qquad (kg\ m^{-3}\ ;\ T_a \text{ in } °C) \qquad (41)$$

Measurements and modeling studies by Schmidt and Gluns (1991) suggest using the average value per unit branch area, $SNLOAD_{branch} = 6.6$ kg m^{-2}, for a pine forest. Furthermore, because the mass balance scheme of the UEB model incorporates SWE depth per unit horizontal surface area, the capacity for snow is found by dividing by the density of water, which yields

$$CAP_S = SNLOAD/\rho_w \qquad (SWE\ m) \qquad (42)$$

The value for a defoliated deciduous forest is not currently known and not considered by Schmidt and Gluns, but likely substantially less than that of pine. Rainfall and snowfall capacities are available from intensive field measurements by Helvey and Patric (1965) and Zinke (1967), which suggest that CAP_R is about one to three times less than CAP_S. Thus the interception sub-model will assume a nominal value of $CAP_R = CAP_S/2$. Furthermore, they indicate that the mean value of CAP_R for coniferous trees, 2 mm, was four times greater than that of defoliated deciduous trees, 0.5 mm, thus CAP_R(coniferous) = $4CAP_R$(defoliated deciduous). The interception sub-model will

provide estimates of sub-canopy snow and rain accumulation at hourly resolution with four input parameters per forest type, including VAI, SVF, $SNLOAD_{branch}$, and u_{crit}. The terms u_{crit} and $SNLOAD_{branch}$ will serve as tuning parameters during evaluation of the interception model.

INDEPENDENT EVALUATION OF THE SUB-MODELS

The sub-models described above were evaluated for the duration of the snow accumulation and melt period observed at UMBS during the period, 1 December 1998 through 31 March 1999. Sub-canopy wind speed at 1.5 m and incoming solar radiation at 1.5 m provide validation data for the solar radiation and wind models. Unfortunately, a lack of resources (instrumentation) precluded measurements of longwave radiation and snowfall interception within the canopy. Nevertheless, it was possible to make comparisons with measurements of above canopy values, which provides a reasonable evaluation of trends and frequency.

Measurement systems

Above canopy and sub-canopy measurement systems were necessary to properly evaluate and validate the performance of the sub-models. Consequently, one of the criteria for choosing UMBS was the availability of above canopy variables for driving a physically based snow model, which also satisfied the sub-model evaluation objective. The measurement system worked nearly flawlessly throughout the season, and any adjustments required during the snow season were minor. Fig. 4 illustrates the test sites at UMBS.

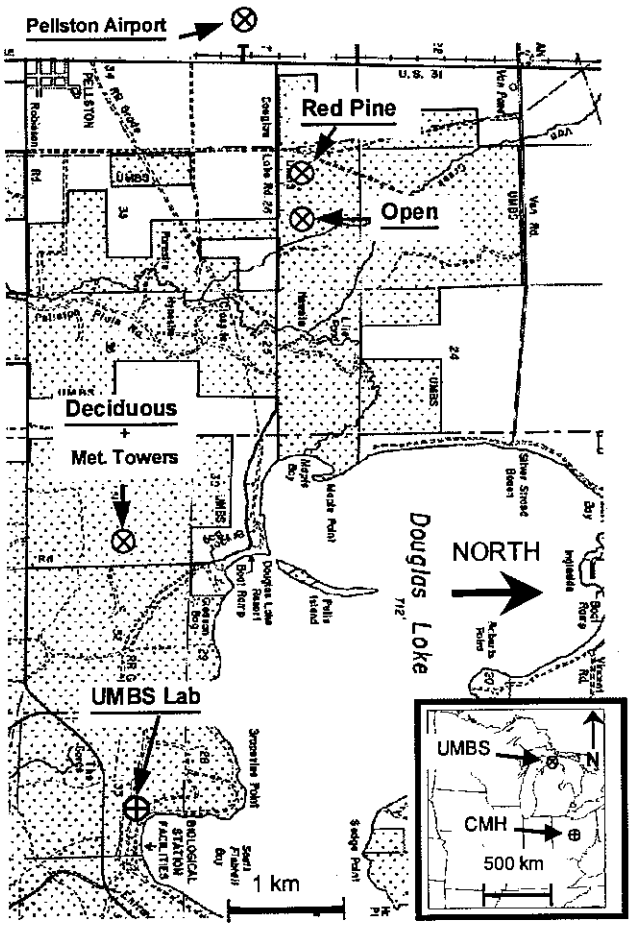

Figure 4. Location map for UMBS and test sites.

Prior to the primary field season, the magnitudes of VAI and SVF were measured utilizing the LICOR LAI-2000 canopy analyzer (LI-COR, 1992) and fish-eye lens photographic techniques (Chazdon and Field, 1987). The LAI-2000, in paired and single sensor modes, provided good repeatability of VAI values for both sites. The results of the measurements are shown in Table 1.

Table 1. Canopy architecture for the defoliated deciduous and red pine sites at UMBS

Forest Type	VAI	SVF
Mixed Deciduous	0.74	0.59
Red Pine	2.63	0.15

An automatic weather station complete with snow stake network was fabricated and deployed at both forest sites prior to the first snowfall. This work required several money-saving strategies, without which Phase I would not have been successful. Fig. 5 illustrates the stake network and instruments connected to a Campbell Scientific CR-7 data logger.

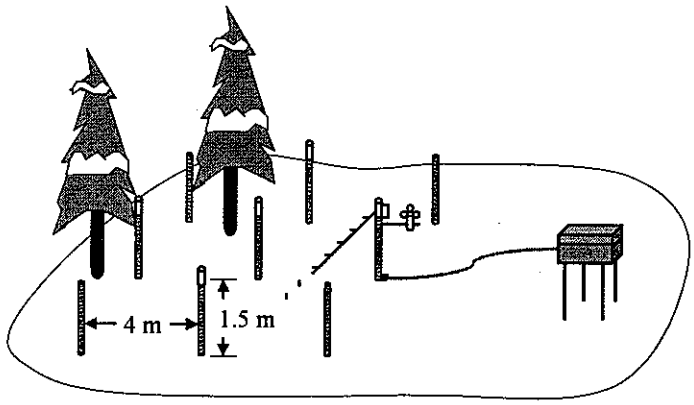

Figure 5. Sub-canopy instrumentation network indicating snow stakes, relative humidity, thermocouple string, anemometer and five radiometers.

Each site maintains nine accumulation stakes evenly spaced over a 8X8 m grid. Five of the stakes supported radiometers sensitive to shortwave radiation. Radiometers were calibrated against an Epply primary standard pyranometer before and after the snow season. For the most part, the radiometers response was linear compared to that of the standard. Radiometers were cheap to build and provided sufficient accuracy, particularly for diffuse radiation; each radiometer consistently underestimated direct solar by about 10%, and linear calibration was used to adjust for this error. A network of five radiometers proved sufficient for providing a measure of the 'average' solar radiation at the forest floor. An effort was made to obtain a random sample of incoming radiation and snow depth within these plots. The average height of both the pine and defoliated decidouous canopies was H = 20m. Above canopy measurements were reduced from one, ten or fifteen minute sampling intervals to obtain hourly averages, which match the hourly averages logged beneath the canopy. Data were collected from the two loggers via laptop computer, roughly every three weeks for the snowcover season, 1 December 1998 to 31 March 1999.

The analysis of Phase I considers weekly periods of good and worst agreement between predicted and observed below-canopy wind (Figs. 6a-b and 7a-b) and solar irradiance (Figs. 8a-b and 9a-b) for the two types of forest.

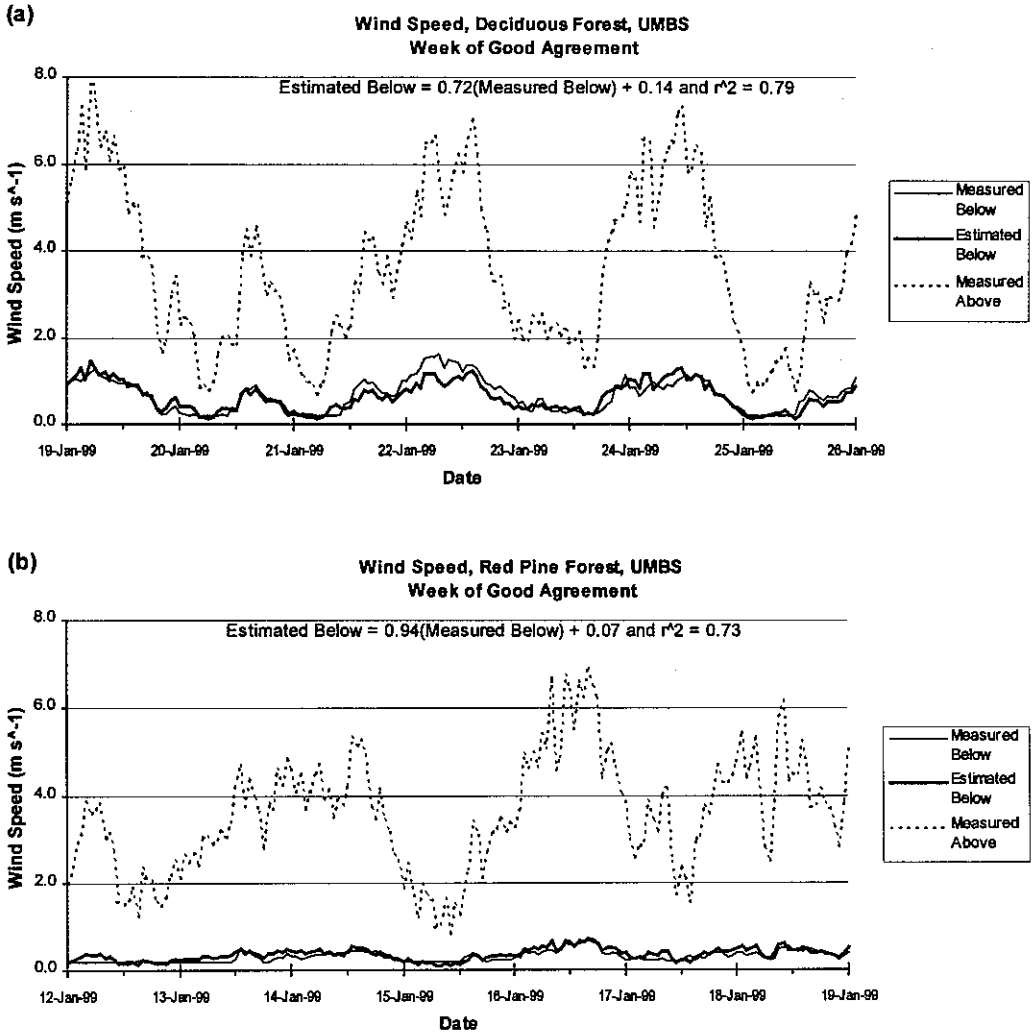

Figure 6. Measured and estimated wind speed for week with good agreement: (a) deciduous site and (b) red pine site. Measured 10 m above canopy height and estimated and measured 1.5 m above forest floor.

Generally, Figs. 6 and 7 suggest substantial reduction of both the magnitude and variability of wind speed for both types of forest. The results in Figs. 6a and 7a indicate that the bluff-body effect of forest cover is significant for canopies with low VAI (and high SVF). Furthermore, results show better agreement when above-canopy wind is higher and its fluctuation is more regular. Agreement is worse, in part, when actual wind speed falls below that of the 0.2 m s^{-1} threshold for the sub-canopy anemometer. This occurs in Fig 7a-b for both types of forest. Note that a "hat" was fixed over the anemometer prior to January; thus, the likelihood of anemometer freezing is reduced. It is possible that the anemometer below the deciduous canopy intermittently froze (Fig. 7a), as the record of precipitation (not shown) suggests a mix of copious amounts of rain and snow-fall during this week in late February. The record indicates no precipitation during the period of worst agreement below the red pine canopy. Nevertheless, the estimation of sub-canopy wind speed is acceptable, considering its substantial reduction compared with that above.

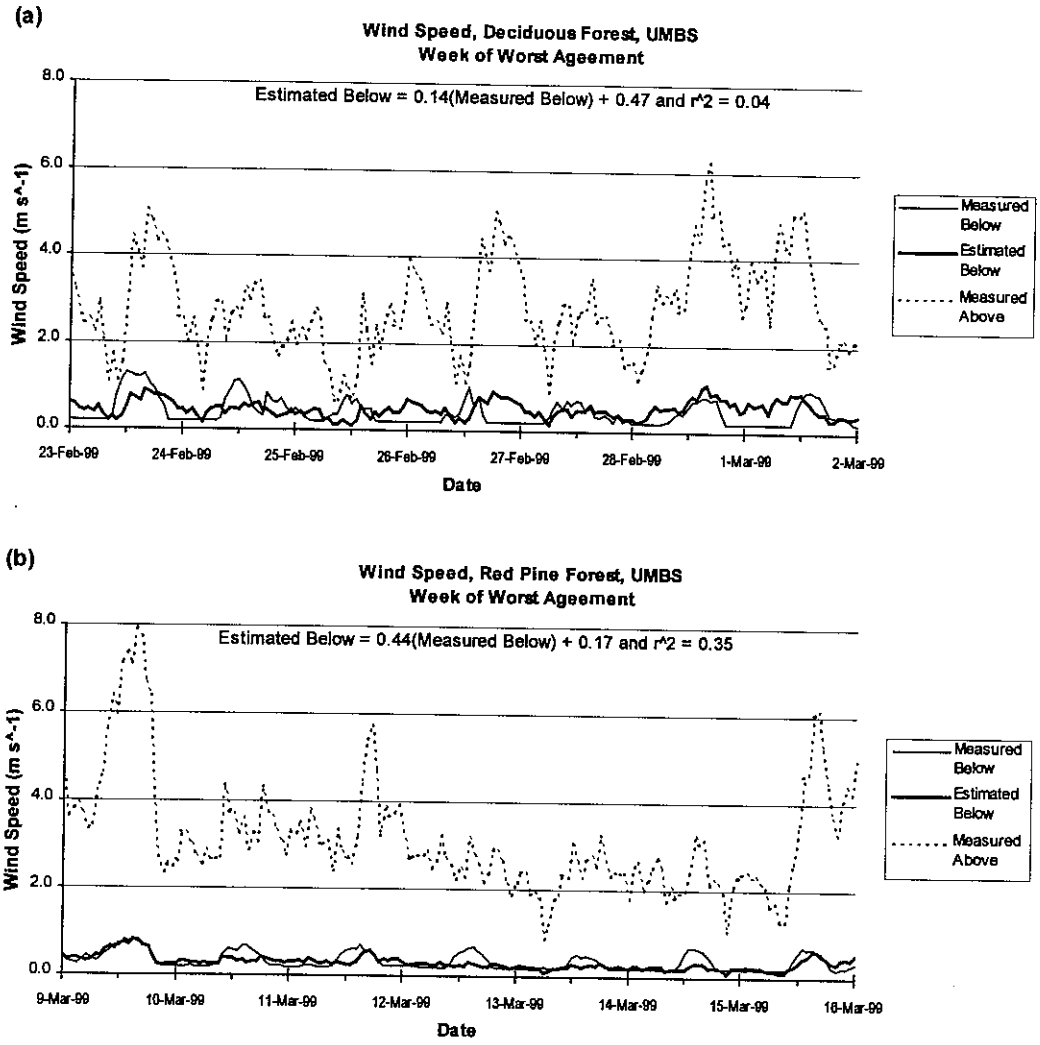

Figure 7. Measured and estimated wind speed for week with worst agreement: (a) deciduous site and (b) red pine site. Measured 10 m above canopy height and estimated and measured 1.5 m above forest floor.

Fig. 8a-b shows substantial reduction in solar irradiance beneath both types of forest cover. Comparison of Figs. 8b and 9b suggests that the estimated irradiance is worse above-canopy values are low, as they are in mid-December. A singularity is apparent in Fig. 8a and 9a and, as indicated by the spike in sub-canopy estimated irradiance. This is likely a result of an inconsistency in the sub-model, which should be resolvable for future applications. It may be a problem due to the VAI<1.0 for the deciduous canopy. For the pine canopy, it appears that solar irradiance is substantially underestimated for lower above canopy measurements (Fig. 7b). Analysis of the remainder of the record suggests that the sub-model consistently underestimates solar irradiance beneath the pine canopy during periods with above-canopy magnitudes less than 200 W m^{-2}. Nevertheless, the sub-model captures the general reduction in solar irradiance for both types of forest.

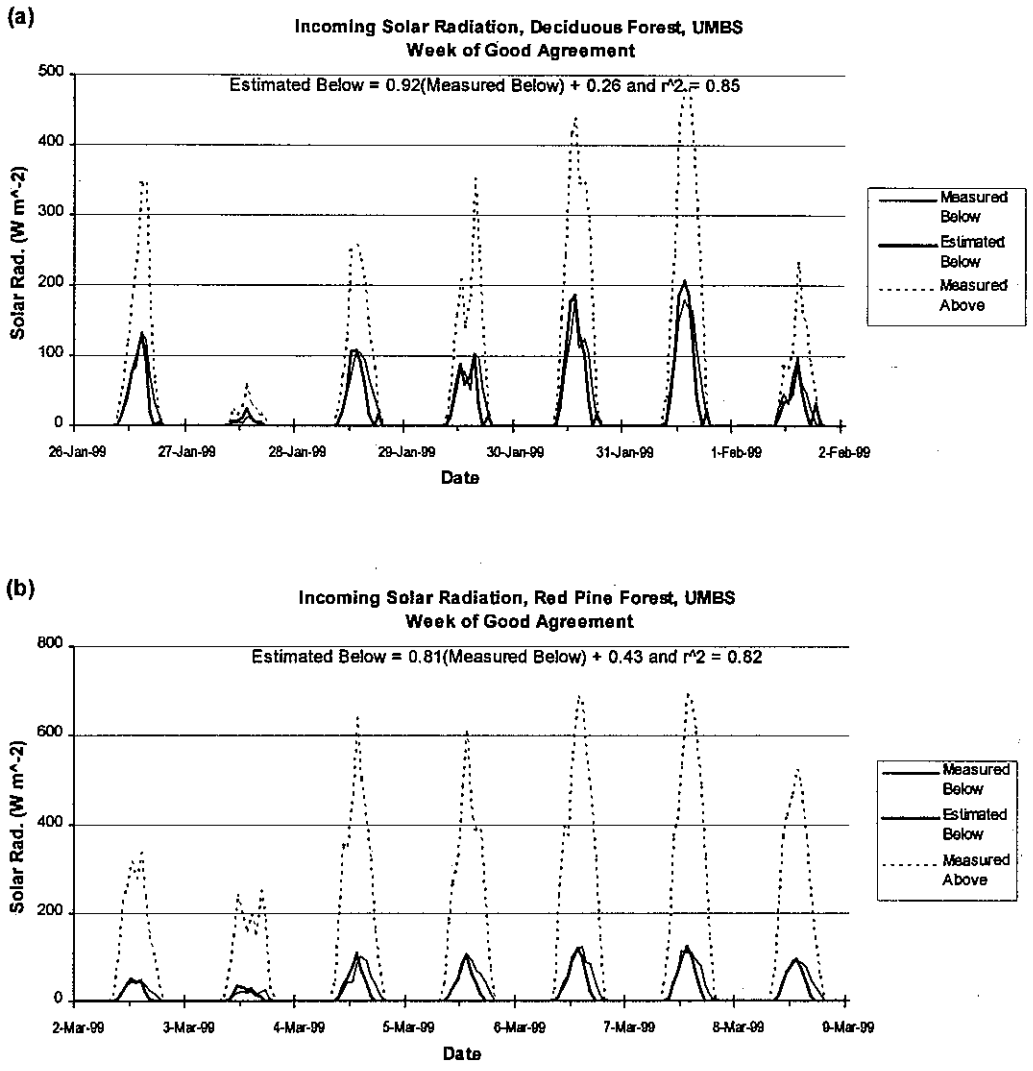

Figure 8. Measured and estimated solar irradiance for week with good agreement: (a) deciduous site and (b) red pine site. Measured 20 m above canopy height and estimated and measured 1.5 m above forest floor.

SUMMARY AND CONCLUSIONS

Based on a review of existing techniques and recent field measurements, this paper developed sub-models for simulation of sub-canopy radiation, wind speed and precipitation, which may be incorporated into remote sensing image interpretation and numerical models. The primary objective of this initial phase was to develop a physically based parameterization, based on available or easily measurable parameters of forest canopy architecture. The intent is to integrate this pragmatic technique into a numerical snowmelt model to improve estimation of both accumulation and melt beneath different types of forest cover. Furthermore, the sub-models were developed for a broad spectrum of end-users, including the climate modeling and remote sensing community. Independent evaluation of the solar radiation and wind sub-models produced favorable results for mature defoliated deciduous and red pine types of forest cover in northern Michigan. Recent completion of Phase I lead to the initiation of Phase II, which will be presented in a follow-up paper in the near future.

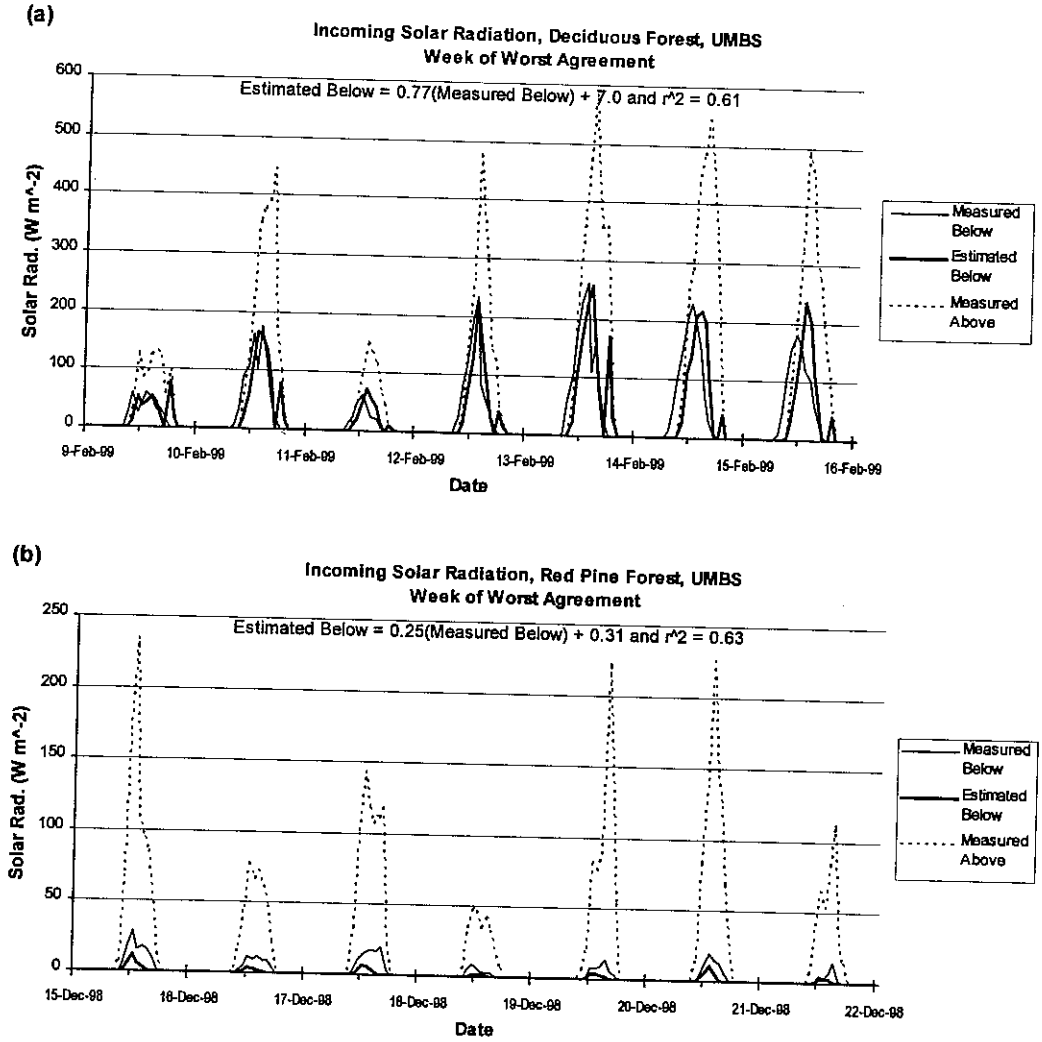

Figure 9. Measured and estimated solar irradiance for week with worst agreement: (a) deciduous site and (b) red pine site. Measured 20 m above canopy height and estimated and measured 1.5 m above forest floor.

ACKNOWLEDGEMENTS

I thank my adviser, John Arnfield, for his intellectual support and encouragement. We had many insightful discussions throughout the fieldwork and writing process that provided the motivation to continue through tuff times.

I thank Peter Curtis, at The Ohio State University, for welcoming me as a collaborator on the AmeriFlux project at University of Michigan Biological Station (UMBS). I am grateful to the winter-over staff at the UMBS for permitting me to use their property, lodging and research facility for my project. Chris Vogel and Bob Vande Kopple provided me with equipment, valuable weather data and moral support.

I thank Dr. Robert Davis, at the Cold Regions Research and Engineering Lab, for his enthusiastic support and helpful suggestions for completing my fieldwork. Bert graciously loaned the fish-eye camera and LAI-2000 canopy analyzer (LI-COR, 1992). I also wish to thank Dr. Mary Anne Carrol in the Department of Atmospheric, Oceanic, and Space Sciences at the University of Michigan and Troy Thornberry for helping with access to weather data from the PROPHET tower at UMBS.

The Graduate Student Alumni Research Award and university Small Grant substantially reduced the cost of travel, lodging and materials for developing the microclimate measurement network.

REFERENCES

Benoit, R. 1977. 'On the integral of the surface layer profile-gradient functions', *J. Appl. Meteor.*, **16**, 859-860.

Berry, G. J., and Rothwell, R. L. 1992. 'Snow ablation in small forest openings in southwest Alberta', *Can. J. For. Res.*, **22**, 1326-31.

Calder, I. R., 1986. 'What are the limits of forest evaporation?—A further comment', *J. Hydrol.*, **89**, 33-36.

Calder, I. R. 1990. *Evaporation in the uplands*. Wiley, Chichester. 144 pp.

Campbell, G. S., and J. M. Norman, 1989: 'The description and measurement of plant canopy struction', in Russel, G., Marshall, B. and Jarvis, P. G. (eds), *Plant Canopies: their growth, from a fuction.* Cambridge University Press, Cambridge, England. pp. 1-19.

Chazdon, R. L., and Field, C. B. 1987. 'Photographic estimation of photosynthetically active radiation: evaluation of a computerized technique', *Oecologia*, **73**, 525- 532.

Cionco, R. M. 1972. 'A wind profile index for canopy flow', *Boundary Layer Meteorol.*, **3**, 255-263.

Domingo, F., Sanchez, G., Moro, M. J., Brenner, A. J., and Puigdefabregas, J. 1998. 'Measurement and modelling of rainfall interception by three simi-arid canopies', *Agric. For. Meteorol.*, **91**, 275-292.

Fassnacht, K. S., Gower, S. T., Norman, J. M., and McMurtrie, R. E. 1994. 'Acomparison of optical and direct methods for estimating foliage surface area index in forests', *Agric. For. Meteorol.*, **71**, 183-207.

Gash, J. H. C., 1979. 'An analytical model of rainfall interception by forests', *Q. J. R. Meteorolog. Soc.*, **105**(443), 43-55.

Hedström, N. R., and Pomeroy, J. W. 1998. 'Measurement and modelling of snow interception in the boreal forest', *Hydrol. Process.*, **12**, 1611-1625.

Helvey, J. D., and Patric, J. H. 1965. 'Canopy and litter interception by hardwoods of rainfall by hardwoods of eastern United States', *Water Resour. Res.*, **1**, 193-206.

Hörmann, G., Branding, A., Clemen, T., Herbst, M., Hinrichs, A., and Thamm, F. 1996. 'Calculation and simulation of wind controlled canopy interception of a beech forest in Northern Germany', *Agric. For. Meteorol.*, 79, 131-148.

Jarvis, P. G., and Leverenz, J. W. 1983. 'Productivity of temperate deciduous and evergreen forests', in Land, O. L., Nobel, P. S., Osmond, C. B., and Ziegler, H. (eds), *Ecosystem processes: mineral cycling, productivity and man's influence.* Springer-Verlag, New York, pp. 233-280.

Jordan, R. 1991. 'A one-dimensional temperature model for a snow cover', *CRREL Spec. Rep. 91-16*, U.S. Army Cold Reg. Res. and Eng. Lab., Hanover, N. H.

Lee, R. 1978. *Forest microclimatology*. Columbia University Press, New York, 276 pp.

Li, X., Straher, A. H., and Woodcock, C. E. 1995. 'A hybrid geometric optical-radiative transfer approach for modeling albedo and directional reflectance of discontinuous canopies', *IEEE Transactions on Geoscience and Remote Sensing*, **33**(2), 466-480.

LI-COR, 1992. LAI-2000: *Plant Canopy Analyzer Operating Manual*, LI-COR, Inc., Lincoln, Nebraska, USA.

Lowe, P. R. 1977. 'An approximating polynomial for the computation of saturation vapor pressure', *J. Appl. Meteorol.*, **16**, 100-103.

Lundberg, A., Calder, I., and Harding, R. 1998. 'Evaporation of intercepted snow: measurement and modelling', *J. Hydrol.*, **206**, 151-163.

Male, D. H., and Granger, R. J. 1981. 'Snow surface energy exchange', *Water Resour. Res.*, 17(3), 609-627.

Massman, W. J. 1983. 'The derivation and validation of a new model for the interception of rainfall by forests', *Agric. Meteorol.*, **28**, 261-286.

McKay, G. A., and Gray, D. M. 1981. 'Distribution of snow cover', in Gray D. M., and Male D. H. (eds), *Handbook of snow, principles, processes, management and use*, Pergamon Press, pp 153-190.

Meyers, T. P., Finkelstein, P., Clark, J., Ellestad, T. G., and Sims, P. F. 1998. 'A multilayer model for inferring dry deposition using standard meteorological measurements', *J. Geophys. Res.*, **103**(D17), 22645-22661.

Monsi, M., and Saeki, T. 1953. 'Uber den lichtfaktor in den pflanzengesellschaften end seine bedeutung fur die stoffproduktion', *Jpn. J. Bot.* **14**, 22-52.

Monteith, J. L. 1975. *Vegetation and the atmosphere. Volume 1, principles*. Academic Press, New York, 278 pp.

Monteith, J. L. 1976. *Vegetation and the atmosphere. Volume 2, case studies*. Academic Press, New York, 439 pp.

Morris, E. M. 1985. 'Snow and ice', in Anderson, M. G., and Burt, T. P. (eds), *Hydrological Forecasting*, John Wiley & Sons Ltd, 153-183.

Nel, E. M., and Wessman, C. A. 1993. 'Canopy transmittance models for estimating forest leaf area index', *Can. J. For. Res.*, **23**, 2579-2586.

Ni, W. 1997. 'A coupled transilience model for turbulent air flow within plant canopies and the planetary boundary layer', *Ag. For. Meteorol.*, **86**, 77-105.

Ni, W., Li, X., Woodcock, C. E., Roujean, J. L., and Davis, R. E. 1997. 'Transmission of solar radiation in boreal conifer forests: Measurements and models', *J. Geophys. Res., Atmospheres*, **102** (D24), 29555-29566.

Nickerson, E. C., and Smiley, V. E. 1975. 'Surface layer and energy budget parameterizations for mesoscale models', *J. Appl. Meteorol.*, **14**. 297-300.

Norman, J. M. 1979. 'Modeling the complete crop canopy', in Barfield, B. J., and Gerber, J. F. (eds), *Modification of the aerial environment of plants*. American Society of Agricultural Engineers, St. Joseph, Mich. pp. 249-277.

Norman, J. M., and Campbell, G. S. 1989. 'Canopy structure', in Pearcy, R. W., Ehleringer, J. R., Mooney, H. A., and Rundel, P. W. (eds), *Plant physiological ecology: field methods and instrumentation*, Chapman and Hall, New York. pp. 301-325.

Pierce, L. L., and Running, S. W. 1988: 'Rapid estimation of coniferous forest leaf area index using a portable integrating radiometer', *Ecology*, 69: 1762-1767.

Pomeroy, J. W., and Dion, K. 1996. 'Winter radiation extinction and reflection in a boreal pine canopy: measurements and modelling', Hydrol. Process., **10**, 1591-1608.

Pomeroy, J. W., Gray, D. M., Shook, K. R., Toth, B., Essery, R. L. H., Pietroniro, A., Hedström, N. 1998. 'An evaluation of snow accumulation and ablation processes for land surface modelling', *Hydrol. Process.*, **12**(15), 2339-2367.

Rutter, A. J., Kershaw, K. A., Robins, P. C., and Morton, A. J. 1971. 'A predictive model of rainfall interception in forest, I, Derivation of the model from observations in a plantation of Corsican pine', *Agric. For. Meteorol.*, **9**, 367-384.

Schmidt, R. A., and Gluns, D. R. 1991. 'Snowfall interception on branches on three conifer species', *Can. J. For. Res.*, **21**, 1262-1269.

Szeicz, G., Petzold, D. E., and Wilson, R. G. 1979. 'Wind in the subarctic forest', *J. Appl. Meteorol.*, **18**, 1268-1274.

Tarboton, D. G., and Luce, C. H. 1997. 'Utah energy balance snow accumulation and melt model (UEB), computer model technical description and users guide', Utah Water Research Laboratory, Utah State University, and USDA Forest Service, Intermountain Research Station, 41 pp. & figures.

U.S. Army Corps of Engineers, 1956. 'Snow Hydrology, summary report of the snow investigations', *U.S. Army Cops Eng., North Pacific Div., Protland, Oreg.*, 437 pp.

Yamaoka, Y. 1958. *Trans. Am. Geophys. Union*, 39, 266-272.

Yamazaki, T.,and Kondo, J. 1992. 'The snowmelt and heat balance in snow-covered forested areas', *J. Appl. Meteorol.*, **31**, 1322-1327.

Zinke, P. J., 1967. 'Forest interception studies in the United States', in Sopper, W. E., and Lull, H. W. (eds), *International Symposium on Forest Hydrology*. New York, Pargamon Press.